EPJ manuscript No.
(will be inserted by the editor)

Monte Carlo nuclear data adjustment via integral information

D. Rochman[1] and E. Bauge[2] and A. Vasiliev[1] and H. Ferroukhi[1] and S. Pelloni[1] and A.J. Koning[3] and J.Ch. Sublet[3]

[1] Paul Scherrer Institut, Villigen, Switzerland
[2] CEA, DAM, DIF, 91297 Arpajon cedex, France
[3] Nuclear Data Section, International Atomic Energy Agency, Vienna, Austria

Received: date / Revised version: date

Abstract. In this paper, we present three Monte Carlo methods to include integral benchmark information into the nuclear data evaluation procedure: BMC, BFMC and Mocaba. They allow to provide posterior nuclear data and their covariance information in a Bayesian sense. Different examples will be presented, among which the case of 14 integral quantities with fast neutron spectra (k_{eff} and spectral indices). Updated nuclear data for ^{235}U, ^{238}U and ^{239}Pu are considered and the posterior nuclear data are tested with MCNP simulations. One of the noticeable outcomes is the reduction of uncertainties for integral quantities, obtained from the reduction of the nuclear data uncertainties and from the rise of correlations between cross sections of different isotopes. Finally, the posterior nuclear data are tested on an independent set of benchmarks, showing the limit of the adjustment methods and the necessity for selecting well representative systems.

PACS. PACS-key describing text of that key – PACS-key describing text of that key

1 Introduction

The improvement of nuclear data (observables such as cross sections, angular and energy spectra) is a continuous activity which is ongoing for many decades. It is justified by the better theoretical knowledge and understanding of the various nuclear reaction processes over the years, and also by the needs from the applied community for improved predictions, reduced costs and enhanced safety. The present paper treats of practical solutions to answer these user needs, by taking into account integral information with Monte Carlo methods in the nuclear data evaluation process.

In spite of the many theoretical advances, the role played by the experimental observations (E) and their uncertainties (ΔE) is still essential in the theoretical predictions of nuclear cross sections. It is guiding the efforts for improving models and calculations (C), but is also used as a calibration tool to adjust model parameters, with the goal to obtain $C - E$ close to 0 within the experimental uncertainties ΔE for the largest number of cases. As a second quantity of interest, the calculated uncertainty ΔC helps to understand the significance of $C-E$ values in context of the model uncertainties (by extension, the "uncertainty" quantity can be replaced by the "covariance" quantity). If ΔC can be assessed, then $C-E$ values being within $0 \pm \sqrt{\Delta E^2 + \Delta C^2}$ (if ΔC and ΔE are uncorrelated) can be seen as a good agreement between C and E. In the following, we will restrict ourselves to ΔC coming from nuclear data as the other sources of uncertainties are outside the scope of this study. In this context, recommended nuclear data are produced using physics-based descriptions in combination with mathematical-based fitting procedures; this is a simplified but illustrative view on the nuclear data evaluation work, and the methods presented in the following are defined with the goal to reduce $C - E$ values, taking into account the experimental and calculated uncertainties.

One of the most convenient source of experimental data for evaluators is the EXFOR database [1], being a collection of E, ΔE, covariance information and related descriptions in various publications. In EXFOR, the vast majority of the E refers to differential measurements, often performed for a single isotope or element, and being independent of the facility spectrum. Such quantities are therefore easily comparable with C coming from a model calculation. And traditionally, evaluators preferred to base their work on clean experiments such as from EXFOR, the result being a so-called general-purpose nuclear data library.

Another important source of experimental knowledge lies in integral information, such as integral benchmarks, as included in the ICSBEP collection [2]. Conceptually, there is little difference in considering differential or integral data to obtain useful information during the evaluation process, but one has to pay attention to possible compensation with integral data, due to the impact of other isotopes included in the model. Additionally, such benchmark systems allow to test the nuclear data in a certain energy

Send offprint requests to:

range, with specific geometries, therefore adding some difficulties in using them in the evaluation process. For these reasons, the integral data have not been mathematically included by evaluators in their procedure, but it is a fact that such data have indirectly been used to perform fine adjustment of specific cross sections to improve the global $C-E$ of an entire library.
With these quantities in hand, it is possible to adjust specific cross sections with mathematical procedures, the results being a posterior set of nuclear data, adjusted for specific applications (*i.e.* taking into account specific integral information). Historically, this adjustment step was not performed by nuclear data evaluators, but by specific users who wanted to derive application libraries based on a general-purpose library. Many methods were developed to perform these adjustments, for instance based on deterministic approaches (see Refs. [3,4] for an extensive description of the various methods), and more recently with Monte Carlo based sensitivity functions [5] and Bayesian methods [6]. Such libraries present some undeniable advantages: better $C-E$ for a specific range of application and smaller ΔC (see for instance Ref. [7,8]). The drawback is nevertheless noticeable: it is to be used for certain applications only (see Ref. [9] for examples on "stress tests" used to test adjusted nuclear data).

Since a few years, two circumstances are pushing to change this accepted evaluation methodology by merging parts of the adjustment methodology into the evaluation process. The first one comes from the user community (criticality-safety, spent fuel management, core simulation) asking for smaller (and justified) uncertainties on calculations for applied quantities. Indeed, by using the covariance information from general-purpose libraries (JEFF, ENDF/B or JENDL), the calculated uncertainties on specific parameters for reactor or fuel are relatively large, and can imply the use of penalty factors. Such uncertainties are now challenged as they do not always correspond to the expert judgment from these large-scale facilities. The second one comes from the evaluator community itself, where it has been recognized that the calculated uncertainties (based on general-purpose libraries) for simple criticality-benchmarks are also too large compared to the experimental uncertainties. Taking these two aspects into consideration, there is nowadays a tendency to shift some of the adjustment work into the evaluation procedure (see *e.g.* Ref. [10]). This would help the user community as they could continue using new library versions such as JEFF, but leading to smaller ΔC and smaller biases. It would also make clearer at the evaluation level which integral benchmarks are in fact considered and how.
It is in this context that this paper presents Monte Carlo solutions to include integral values into the evaluation procedure. Whereas there are a few existing deterministic methods to obtain such adjustments, Monte Carlo methods are becoming more attractive as computer power is more available than before, and as less assumptions are necessary compared to specific deterministic methods. In the following, we will first present the different necessary quantities (section 2), followed by the three Monte Carlo methods (sections 3 to 5). Contrary to Ref. [5], the presented methods do not use sensitivity vectors. Specific sections will present the practical solution of making an evaluation from these posterior nuclear data (section 6) and the issues of convergence linked to Monte Carlo methods (section 7). Finally, results will be presented considering 14 integral quantities: for posterior $C-E$, posterior nuclear data and covariance, and examples of the predictive power (or stress tests) for these updated quantities will also be presented.

2 General description

This work is based on Monte Carlo sampling and a repetition of the same integral (benchmark) calculations with randomly chosen inputs (specific nuclear data), thus avoiding the explicit use of sensitivity vectors (or coefficients). These inputs are the nuclear data evaluations for three isotopes: ^{238}U, ^{235}U and ^{239}Pu. As previously presented in many publications, a random nuclear data file, for instance for ^{238}U, is produced by randomly choosing the model parameters (such as in TALYS) and the resonance parameters, according to specific probability density functions (pdf). In this work, all parameters are independently sampled, following Normal distributions with specific standard deviations. Such standard deviations are selected to globally reproduce experimental differential data, such as in EXFOR. Additionally, the resonance range is not modified as this study concentrates on systems driven by fast neutrons only. The next sections will present some details on the considered nuclear data and the integral benchmarks. For readers more interested on the generation of the random nuclear data, we refer to the extensive description from Ref. [11].

2.1 Nuclear data

In the following we will consider a set of random nuclear data evaluations for each isotope, in practice represented by ENDF-6 files [12] which contain all cross sections and spectra. For simplicity, such random nuclear data evaluations will be called $^{235}\mathrm{U}_i$ for the i^{th} random realization of the ^{235}U nuclear data, and similar notation will be used for the other isotopes such as ^{238}U or ^{239}Pu. $^{235}\mathrm{U}_i$ is a vector (or a set of long tables in an ENDF-6 file) containing all the important nuclear data represented with the symbol σ: cross sections (fission, scattering, *etc*), spectra (such as prompt fission neutron spectra), number of fission neutrons (prompt $\overline{\nu}$), but also angular distributions and other. All these quantities are represented as a function of the incident (and if necessary outgoing) neutron energy E_{inc}. In general, E_{inc} varies from 0 to 20 MeV.

Such random nuclear data set is expressed as follows:

$$^{235}\mathbf{U_i} = \begin{bmatrix} \sigma 1(E_{\rm inc})_i \\ \sigma 2(E_{\rm inc})_i \\ \vdots \\ \sigma n(E_{\rm inc})_i \end{bmatrix} \quad (1)$$

The number of random files i will vary from 1 to I, I being 10 000 in this work. In the following, the term $(E_{\rm inc})$ is not repeated and $\sigma 1(E_{\rm inc})_i$ will be simply noted $\sigma 1_i$. n is a large number referring to energy and reaction dependent nuclear data: for elastic, fission, inelastic cross sections and so on.
As for any distribution of observables, different moments of the distribution of the I quantities can be obtained, such as the average $\overline{\sigma 1}$, the variance var($\sigma 1$) or the covariance term between two nuclear data cov($\sigma 1, \sigma 2$):

$$\overline{\sigma 1} = \frac{1}{I}\sum_i^I \sigma 1_i \quad (2)$$

$$\text{var}\,(\sigma 1) = \frac{1}{I}\sum_i^I (\sigma 1_i - \overline{\sigma 1})^2 \quad (3)$$

$$\text{cov}\,(\sigma 1, \sigma 2) = \frac{1}{I}\sum_i^I (\sigma 1_i - \overline{\sigma 1})(\sigma 2_i - \overline{\sigma 2}) \quad (4)$$

It is understood that all these quantities can be defined for specific neutron energies $E_{\rm inc}$. A useful quantity in the following is the covariance matrix for the nuclear data, called $\mathbb{M}_\sigma$, simply being

$$\mathbb{M}_\sigma = \begin{bmatrix} \text{cov}\,(\sigma 1, \sigma 1) & \text{cov}\,(\sigma 1, \sigma 2) & \dots \\ \vdots & \ddots & \\ \text{cov}\,(\sigma n, \sigma 1) & & \text{cov}\,(\sigma n, \sigma n) \end{bmatrix} \quad (5)$$

where cov$(\sigma 1, \sigma 2)$ is presented in Eq. (4).
In the present work, the nuclear data are considered for a limited number of energies, using 68 groups from 4 keV to 20 MeV. These groups are a subset of the 187 groups as defined in Ref. [13]. Such energy range is adequate given the choice of benchmarks (see next section). Additionally, a limited number of reactions is considered for practical reasons: (n,el), (n,γ), (n,f), (n,inl) (from the first inelastic level to the 20$^{\rm th}$, including the continuum), $\overline{\nu}_{\rm prompt}$ (later called $\overline{\nu}$) and five fission neutron spectra for the incident neutron energies from 200 keV to 3 MeV. It represents a total of 30 reaction channels, leading to a vector of $n = 30 \times 68 = 2040$ numbers for a single isotope.
For the benchmarking presented in section 2.2, the 3 main isotopes ^{238}U, ^{235}U and ^{239}Pu are represented with I = 10 000 random files each. This number is chosen so that the different calculated Monte Carlo moments are converged in a satisfactory manner, see for example Ref. [14]. There is therefore I^3 possible combinations of random vectors ($^{\mathbf{238}}\mathbf{U_i}$, $^{\mathbf{235}}\mathbf{U_{i'}}$, $^{\mathbf{239}}\mathbf{Pu_{i''}}$). As this number is relatively high given the computational resources, we will consider only I possibilities where $i = i' = i''$. As these isotopic random nuclear data evaluations were independently produced using different random numbers (in fact different seeds for the random number generators), this choice is an arbitrary but representative subset of the possibilities. For a specific value of i, the nuclear data will be represented by the vector $\mathbf{ND_i}$ such as:

$$\mathbf{ND_i} = \begin{bmatrix} ^{\mathbf{235}}\mathbf{U_i} \\ ^{\mathbf{238}}\mathbf{U_i} \\ ^{\mathbf{239}}\mathbf{Pu_i} \end{bmatrix} \quad (6)$$

It contains all the necessary random nuclear data (cross sections and others) for each of the three isotopes, and is therefore of large dimension: for the three isotopes together, the number of elements of $\mathbf{ND_i}$ is $3 \times 2040 = 6120$. (in practice, such data for each isotope can be formatted into a so-called ACE file, being of tens of Mb each). The set of I = 10 000 random nuclear data is represented by the vector $\boldsymbol{\Sigma}$:

$$\boldsymbol{\Sigma} = \begin{bmatrix} \mathbf{ND_1} \\ \vdots \\ \mathbf{ND_I} \end{bmatrix} \quad (7)$$

In the present case, the dimension of the vector $\boldsymbol{\Sigma}$ is $N = 6120 \times 10\,000 = 6.12 \times 10^7$.
As presented later, it is useful to define the nuclear data average $\overline{\mathbf{ND}}$, being simply the arithmetic average of the I random cases:

$$\overline{\mathbf{ND}} = \begin{bmatrix} \overline{^{\mathbf{235}}\mathbf{U}} \\ \overline{^{\mathbf{238}}\mathbf{U}} \\ \overline{^{\mathbf{239}}\mathbf{Pu}} \end{bmatrix} \quad (8)$$

Each element represented under $\overline{^{\mathbf{235}}\mathbf{U}}$ is defined by Eq. (2). The dimension of $\overline{\mathbf{ND}}$ is the same as $\mathbf{ND_i}$: 6120. In the following, the vector of dimension $1 \times n$ will be presented with bold letters, such as $\mathbf{ND}$, whereas matrices of larger dimensions $m \times n$ will be presented in the "AMS math symbol font B", such as $\mathbb{M}$. Also, the subscripts (*e.g.* $_i$) will refer to the i$^{\rm th}$ random file, and the superscripts (*e.g.* $^{(p)}$) will refer to the experimental case.

2.2 Benchmarking

In the following equations, i will also refer to a random MCNP6 calculation for a set of different benchmarks, using the random nuclear data $\mathbf{ND_i}$. Such calculation i is based on a particular set of random ACE files, one for each of the 3 isotopes ^{235}U, ^{238}U and ^{239}Pu. Thus, i will correspond to the three random files and the results of the MCNP6 calculation for each of the P integral quantities. Such calculation process can be represented by the

following scheme:

$$\mathbf{ND_i} = \begin{bmatrix} {}^{235}\mathbf{U_i} \\ {}^{238}\mathbf{U_i} \\ {}^{239}\mathbf{Pu_i} \end{bmatrix} \xrightarrow{\text{MCNP6}} \begin{bmatrix} \mathrm{q}^{(1)}_{\mathrm{calc,i}} \\ \mathrm{q}^{(2)}_{\mathrm{calc,i}} \\ \vdots \\ \mathrm{q}^{(p)}_{\mathrm{calc,i}} \\ \vdots \\ \mathrm{q}^{(P)}_{\mathrm{calc,i}} \end{bmatrix} = \mathbf{Q_{calc,i}} \quad (9)$$

A vector $\mathbf{ND_i}$ can be used to calculate a number of benchmarks with different quantities such as $\mathrm{k_{eff}}$ or spectral indices (the index "calc" denotes a calculated quantity, contrary to "exp" which means an experimental quantity). These calculated quantities are of a total of P for a given i, and p is their index (from 1 to P). In a more general notation, Eq. (9) is equivalent to

$$\mathbf{Q_{calc,i}} = f\left(\mathbf{ND_i}\right), \quad (10)$$

where f is a function representing the integral benchmark calculation using the nuclear data set $\mathbf{ND_i}$. In this representation $\mathbf{Q_{calc,i}}$ is a vector of P values and each value is obtained from the run i with the nuclear data $\mathbf{ND_i}$. One can notice in general that $P \ll n$, implying that even if not all elements of $\mathbf{ND_i}$ are relevant for the calculations of $\mathbf{Q_{calc,i}}$, a large number of random cases will be necessary to obtain meaningful posterior distributions.

In the following, it is also useful to define the vector $\overline{\mathbf{Q_{calc}}}$, still containing P values, but this time each value being the average of the I calculations for each p integral quantity.

In a more general form, we can define the vector $\mathbf{Q_{calc}}$ containing all the values of $\mathbf{Q_{calc,i}}$ for i from 1 to I. In this case, Eq. (10) is equivalent to

$$\mathbf{Q_{calc}} = f\left(\boldsymbol{\Sigma}\right), \quad (11)$$

In the present work, f is a MCNP6 calculation, and $P = 14$ integral quantities, coming from 12 specific benchmarks, as listed in Table 1. Three quantities are used: $\mathrm{k_{eff}}$ and two spectral indices F28/F25 and F49/F25, corresponding to the ratios of the fission rates per atom for ^{238}U and ^{239}Pu over ^{235}U, respectively. Each benchmark name follows the usual nomenclature of the ICSBEP database: 3 letters followed by numbers. All benchmarks are metallic (given by the second letter) and are sensitive to the fast neutron range (given by the third letter). The benchmark names starting with a "p" refer to plutonium systems, the ones starting with a "h" refers to ^{235}U benchmarks, "i" means a mixture of ^{235}U and ^{238}U, and "m" means a mixture of ^{235}U, ^{238}U and ^{239}Pu isotopes. The experimental values are later represented by the vector $\mathbf{Q_{exp}}$ of dimension $P = 14$ and the experimental uncertainties are represented by a similar vector $\boldsymbol{\Delta}\mathbf{Q_{exp}}$.

A quantity used in the following is the benchmark experimental covariance matrix, called $\mathbb{M}_\mathbf{e}$. It is a square matrix, of dimension P×P, filled with element

$$\rho_{p,j} \times \Delta \mathrm{q}^{(p)}_{\mathrm{exp}} \Delta \mathrm{q}^{(j)}_{\mathrm{exp}}$$

Table 1. List of the considered experimental values (14) from 12 criticality benchmarks. The measured values are the ones reported in Ref. [2]. "name" is the benchmark name.

p	name	surname	quantity	measurement
1	imf1-1	Jemima	$\mathrm{k_{eff}}$	0.99880 ± 90 pcm
2	imf7	Bigten	$\mathrm{k_{eff}}$	1.00450 ± 70 pcm
3	mmf1		$\mathrm{k_{eff}}$	1.00000 ± 160 pcm
4	pmf2	Jezebel-40	$\mathrm{k_{eff}}$	1.00000 ± 200 pcm
5	pmf1	Jezebel	$\mathrm{k_{eff}}$	1.00000 ± 200 pcm
6	pmf1		F28/F25	0.2133 ± 0.0023
7	mmf3		$\mathrm{k_{eff}}$	0.99930 ± 160 pcm
8	hmf1		F49/F25	1.4152 ± 0.0140
9	pmf22		$\mathrm{k_{eff}}$	1.00000 ± 210 pcm
10	hmf28	Flattop-25	$\mathrm{k_{eff}}$	1.00000 ± 300 pcm
11	imf2	Pajarito	$\mathrm{k_{eff}}$	1.00000 ± 300 pcm
12	pmf6	Flattop-Pu	$\mathrm{k_{eff}}$	1.00000 ± 300 pcm
13	pmf6		F28/F25	0.1799 ± 0.0020
14	pmf8	Thor	$\mathrm{k_{eff}}$	1.00000 ± 60 pcm

There are different ways of evaluating the matrix $\mathbb{M}_\mathbf{e}$. The uncertainties $\Delta \mathrm{q}^{(p)}_{\mathrm{exp}}$ directly come from the ICSBEP evaluation database (or in a general manner from any integral database such as IRPhe, SINBAD [15], or differential as EXFOR), whereas there is no consensus on the the correlation coefficients $\rho_{p,j}$ (see Refs. [3,16] for details). These correlation coefficients are not provided in Ref. [2] and international efforts are ongoing to establish such values for the most important benchmarks [17–19]. In this work, we consider the 14 experimental values uncorrelated. Considering only two measured quantities, $\mathbb{M}_\mathbf{e}$ is simply:

$$\mathbb{M}_\mathbf{e} = \begin{bmatrix} (\Delta \mathrm{q}^{(1)}_{\mathrm{exp}})^2 & 0 \\ 0 & (\Delta \mathrm{q}^{(2)}_{\mathrm{exp}})^2 \end{bmatrix} \quad (12)$$

with the $\Delta \mathrm{q}^{(p)}_{\mathrm{exp}}$ values given in Table 1. Such approximation has no consequence on the goal of this paper which is the demonstration of the applicability of the Monte Carlo adjustment methods.

Finally, it is also possible to define the $\mathbb{M}_\mathbf{c}$ matrix, being the prior covariance matrix for the calculated integral quantities. Such matrix can easily be defined as

$$\mathbb{M}_\mathbf{c} = \begin{bmatrix} \mathrm{cov}_{c\ 1,1} & \mathrm{cov}_{c\ 1,2} & \cdots \\ \vdots & \ddots & \\ \mathrm{cov}_{c\ P,1} & & \mathrm{cov}_{c\ P,P} \end{bmatrix} \quad (13)$$

where

$$\overline{\mathrm{q}^{(p)}_{\mathrm{calc}}} = \frac{1}{I} \sum_i^I \mathrm{q}^{(p)}_{\mathrm{calc},i} \quad (14)$$

$$\mathrm{cov}_{c\ 1,2} = \frac{1}{I} \sum_i^I (\mathrm{q}^{(1)}_{\mathrm{calc},i} - \overline{\mathrm{q}^{(1)}_{\mathrm{calc}}})(\mathrm{q}^{(2)}_{\mathrm{calc},i} - \overline{\mathrm{q}^{(2)}_{\mathrm{calc}}}) \quad (15)$$

The correlation terms between two benchmarks can be defined as follows: $\rho_{1,2} = \frac{\mathrm{cov}_{c\ 1,2}}{\sqrt{\mathrm{cov}_{c\ 1,1} \times \mathrm{cov}_{c\ 2,2}}}$, and are presented in Fig. 1 in the case of $I = 10\,000$ random files for

the three considered isotopes. This correlation matrix is used later for the BMC, BFMC and Mocaba methods and the calculated standard deviations are given by the diagonal elements of the equivalent covariance matrix. Due

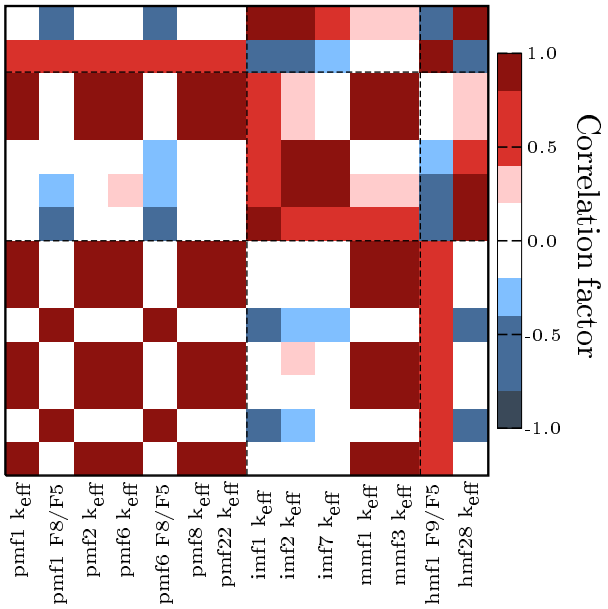

Fig. 1. Prior correlation matrix $\mathbb{M}_\mathbf{c}$ for the 14 benchmark quantities. Such matrix is produced using I random files for ^{235}U, ^{238}U and ^{239}Pu. F5, F8 and F9 means F25, F28 and F29 respectively.

to the selection of benchmarks, this matrix can be subdivided in three groups: the plutonium benchmarks, the ^{235}U highly enriched benchmarks, and in between. In general, the correlation factors are relatively high, as between the k_{eff} for the plutonium benchmarks. The spectral indices F28/F25 are weakly correlated with the k_{eff} and strongly correlated between themselves. Also, the F49/F25 for the hmf1 benchmark is strongly correlated with all the plutonium k_{eff}. The imf benchmarks, which do not contain ^{239}Pu, are not correlated with the pmf k_{eff}, but present some non negligible correlations with the pmf spectral indices. These correlations, coming from the nuclear data only, do not include the covariance information from other sources.

3 BMC/BFMC equations

The BMC and BFMC methods were already presented in a few papers [20,14,21–23] and only the necessary equations are repeated here. One can notice that the BMC method is very close to the UMC-B description as presented in Refs. [24,25].

3.1 χ^2 definition

χ^2 is a very convenient integral quantity to compare performances of calculations with experimental values. As presented in Ref. [26], a general description of χ^2 for the i realization of the nuclear data is

$$\chi^2_i = [\mathbf{Q_{exp}} - \mathbf{Q_{calc,i}}]^T \, \mathbb{M}_\mathbf{e}^{-1} \, [\mathbf{Q_{exp}} - \mathbf{Q_{calc,i}}] \qquad (16)$$

where the superscript ^{T} means the transpose of the vector or matrix and the superscript $^{-1}$ means its inverse. The definitions of the different vectors and matrices are given in the previous sections. As mentioned earlier, the prior correlation terms between the benchmarks are not well-known and they are assumed here to be all zero. In this case, the matrix $\mathbb{M}_\mathbf{e}$ is reduced to a simple expression (similar to Eq. (12)) and when divided by the degree of freedom P, Eq. (16) is equivalent to

$$\chi^2_i/P = \frac{1}{P}\sum_p^P \left(\frac{q^{(p)}_{calc,i} - q^{(p)}_{exp}}{\Delta q^{(p)}_{exp}} \right)^2 \qquad (17)$$

The value calculated with Eq. (17) directly indicates how far are the calculations i from the measurements in terms of average standard deviation. It is worth noting that a value close to 1 indicates a "sufficient" agreement; there is no need from a statistical point of view to obtain $\chi^2_i/P = 0$, which could indicate an "over calibration" (tuning of nuclear data) to the P benchmark values.

3.2 Weight definition

Based on the above definition of χ^2_i for a specific realization i of the vector $\mathbf{Q_{calc,i}}$ (random nuclear data), the BMC and BFMC methods are using different definitions of weights, called w_i. Such weights reflect the agreement between the calculated and measured values: if the agreement of the random case i with the P experimental values is better than for the random case i', the weight attached to the random vector $\mathbf{Q_{calc,i}}$ will be higher than the one for $\mathbf{Q_{calc,i'}}$. The expression of the weight for BMC is

$$w_i = \exp(-\frac{\chi^2_i}{2}) \qquad (18)$$

Such weight is directly proportional to the likelihood function. It can be observed that the values of w_i will change if Eq. (16) or Eq. (17) is considered, but the method stays the same. The calculation of the $q_{calc,i}$ values is the most time-consuming process in this method, but once it is done, w_i can be easily (re)calculated with different definitions. In the case of the BFMC method, the definition of the weights w_i is different. Because of approximations in the reaction models, of simplifications and assumptions in the calculations of the χ^2_i values, Eq. (18) can lead in practice to extremely small weights. The alternative proposed by the BFMC method is to change the value in the exponential so that the spread of the χ^2_i does not lead to extreme variations of weights. This is achieved by renormalizing χ^2_i values, for instance such as:

$$w_i = \exp(-\frac{\chi^2_i}{\chi^2_{min}}) \qquad (19)$$

where $\chi^2_{\rm min}$ is the minimum χ^2 value obtained within the I random cases. One can notice that in Ref. [27], an additional square is used. This is again to empirically avoid a large dispersion of weights. From a practical approach, such normalizations and change of weight definition can be performed in an *ad hoc* way and can be justified by different model defects in the calculation of χ^2_i. The definition of Eq. (19) does not correspond to a Bayesian one anymore, but allows to obtain weights which are not too small in the case of relatively large spread of weights (see Ref. [27] for a comparison of the different evaluation methods based on Monte Carlo sampling). The weight definition is the only difference between BMC and BFMC. As presented in the following, it will have a strong impact on the results, mainly because many weights w_i are extremely small in the case of BMC.

3.3 Updating the prior

As explained, a weight w_i is assigned to a specific nuclear data such as $\sigma 1_i$. Therefore, the posterior nuclear data in terms of average, variance and covariance are defined in a very similar way compared to Eqs. (2) to (4):

$$\overline{\sigma 1}' = \frac{1}{\omega}\sum_i^I \sigma 1_i \times w_i \quad (20)$$

$$\mathrm{var}\,(\sigma 1)' = \frac{1}{\omega}\sum_i^I \left((\sigma 1_i - \overline{\sigma 1}')^2 \times w_i\right) \quad (21)$$

$$\mathrm{cov}\,(\sigma 1, \sigma 2)' = \frac{1}{\omega}\sum_i^I (\sigma 1_i - \overline{\sigma 1}')(\sigma 2_i - \overline{\sigma 2}') \times w_i \quad (22)$$

with

$$\omega = \sum_i^I w_i \quad (23)$$

(note that the $'$ is used in these expressions to represent posterior values). Similar to the definition of Eq. (8), Eq. (20) allows to define an updated average $\overline{\mathbf{ND}}'$, being a vector of different $\overline{\sigma_i}'$ with updated covariance vectors. Eq. (22) is the posterior of nuclear data covariance, defined in a matrix form as $\mathbb{M}_\sigma{}'$.

The BMC and BFMC methods then offer posterior values for the three mentioned quantities, taking into account P integral data. As for any Monte Carlo process, one has to assure that these quantities are converged in a statistical sense. For an unweighted distribution of observables, the rate of convergence follows a $1/\sqrt{i}$ function, whereas different options exist for weighted distributions [28]. Specific convergence rates will be presented in section 7.

In a similar way, the calculated benchmark values can be updated using a weighted average:

$$\overline{\mathrm{q}^{(\mathrm{p})}_{\mathrm{calc}}}' = \frac{1}{\omega}\sum_i^I \mathrm{q}^{(\mathrm{p})}_{\mathrm{calc,i}} \times w_i \quad (24)$$

Eq. (24) can be applied for each of the P benchmarks, leading to P updated averaged benchmark values $\overline{\mathbf{Q_{calc}}}'$, corresponding to the updated average nuclear data $\overline{\boldsymbol{\Sigma}}'$. As for Eq. (11), we can express the update procedure with the following equation:

$$\overline{\mathbf{Q_{calc}}}' = f\left(\overline{\boldsymbol{\Sigma}}'\right), \quad (25)$$

where the updated values correspond to averages (for both nuclear data and integral values). One can notice that there is no need to define a covariance matrix between the calculated quantities and the nuclear data to obtain posterior cross sections. Such matrix is implicit in the use of the weights w_i. As presented in the next section, the Mocaba approach is explicitly using this matrix.

In order to compare the posterior and prior results, Table 2 presents the calculated prior benchmark values, both from the average of the I random runs, and for the nominal set of ENDF files, called "file 0". The "file 0" is obtained from the set of nominal model parameters, without random variations. It corresponds to the best-estimate calculation for the nuclear data (cross sections and other) as one can find in a nuclear data library. For later comparison, the simplified χ^2 divided by the degree of freedom with the average biases (sum of the $\overline{\mathrm{C}}-E$ or of the absolute values of $\overline{\mathrm{C}}-E$, $\sum$ and $\sum||$, respectively) are also indicated. This table is pointing out the difference between the nominal file (file 0) and the average of the I random files: showing that the calculated integral values are different for $\mathbf{ND_0}$ and $\overline{\mathbf{ND}}$. This table also indicates that almost all differences $\overline{\mathrm{C}}-E$ can be covered by ΔC. It also does not mean that an adjustment of nuclear data can

Table 2. List of considered benchmarks with the calculated prior $\overline{\mathrm{C}}-E$ integral values. Values in red and orange are outside 2 and 1 experimental standard deviations, respectively. Values in black are within one standard deviation. All values are given in terms of values $\times 10^5$.

			ΔE	$\overline{\mathrm{C}}-E \pm \Delta$C average	C-E file 0
1	imf1	$k_{\rm eff}$	90	-91 ± 910	+363
2	imf7	$k_{\rm eff}$	70	-292 ± 850	-153
3	mmf1	$k_{\rm eff}$	160	-132 ± 670	+3
4	pmf2	$k_{\rm eff}$	200	+329 ± 670	+440
5	pmf1	$k_{\rm eff}$	200	+77 ± 780	+162
6	pmf1	F28/F25	230	-394 ± 540	-230
7	mmf3	$k_{\rm eff}$	160	+117 ± 640	+280
8	hmf1	F49/F25	1400	-2680 ± 2530	-2730
9	pmf22	$k_{\rm eff}$	210	-85 ± 796	+13
10	hmf28	$k_{\rm eff}$	300	+309 ± 932	+686
11	imf2	$k_{\rm eff}$	300	-238 ± 835	+8
12	pmf6	$k_{\rm eff}$	300	+478 ± 777	+559
13	pmf6	F28/F25	200	-301 ± 424	-40
14	pmf8	$k_{\rm eff}$	60	-192 ± 734	-126
		$\sum\|\|/P$		414 ± 480	414
		$\sum/P$		-54 ± 480	-55
		χ^2/P		3.3	3.4

simultaneously reduce all $\overline{\mathrm{C}} - E$ to zero, but it indicates a possible degree of improvement. One can see that only 5 calculated integral values are within one experimental standard deviation, being 36 % of all integral values.
As an additional indication of the deviation between calculated and measured integral values, the average deviations are also indicated with an uncertainty of 480 pcm. It is obtained using the calculated uncertainties ΔC on each integral values, and with the correlation matrix presented in Fig. 1. Because of the non negligible correlation terms in $\mathbb{M}_{\mathbf{c}}$, the calculated global uncertainty is smaller than the individual components.

4 Mocaba equations

The Mocaba equations presented in the following were already introduced in two papers, see Refs. [32,33]. They are summarized below, keeping the same notation as for the BMC/BFMC equations.

4.1 Definitions

Four equations are necessary to define the posterior nuclear data and integral quantities and their covariance matrices.

$$\overline{\mathbf{Q_{calc}}}' = \overline{\mathbf{Q_{calc}}} + \mathbb{M}_{\mathbf{c}}(\mathbb{M}_{\mathbf{c}} + \mathbb{M}_{\mathbf{e}})^{-\mathbf{1}} \times \left(\mathbf{Q_{exp}} - \overline{\mathbf{Q_{calc}}}\right) \quad (26)$$

$$\mathbb{M}_{\mathbf{c}}{}' = \mathbb{M}_{\mathbf{c}} - \mathbb{M}_{\mathbf{c}}(\mathbb{M}_{\mathbf{c}} + \mathbb{M}_{\mathbf{e}})^{-\mathbf{1}}\mathbb{M}_{\mathbf{c}}{}^{\mathbf{T}} \quad (27)$$

$$\overline{\mathbf{ND}}' = \overline{\mathbf{ND}} + \mathbb{M}_{\sigma,\mathbf{c}}(\mathbb{M}_{\mathbf{c}} + \mathbb{M}_{\mathbf{e}})^{-\mathbf{1}} \times \left(\mathbf{Q_{exp}} - \overline{\mathbf{Q_{calc}}}\right) \quad (28)$$

$$\mathbb{M}_{\sigma}{}' = \mathbb{M}_{\sigma} - \mathbb{M}_{\sigma,\mathbf{c}}(\mathbb{M}_{\mathbf{c}} + \mathbb{M}_{\mathbf{e}})^{-\mathbf{1}}\mathbb{M}_{\sigma,\mathbf{c}}{}^{\mathbf{T}}. \quad (29)$$

As before, $\mathbf{Q_{exp}}$ represents the experimental values from the selected benchmarks, and $\overline{\mathbf{Q_{calc}}}$ is also a vector of 14 values, each of them being the average of the $I = 10\ 000$ random cases. $\overline{\mathbf{Q_{calc}}}'$ represents the updated average values, similar to Eq. (25) in the BMC case. The $\mathbb{M}_{\mathbf{e}}$ matrix is the same as previously defined with non-zero diagonal elements only (no uncertainties from the methods are included). In Eq. (27), all the terms are similar to the BMC description for $\mathbb{M}_{\mathbf{c}}$ and $\mathbb{M}_{\mathbf{c}}{}'$. Both Eqs. (26) and (27) are enough to define the posterior distribution for the calculated integral quantities. Their counterparts in the BMC/BFMC approach are the Eqs. (20), (22) and (24).
The two following equations (28 and 29) define the posterior distributions for the nuclear data. An additional matrix is necessary compared to BMC, corresponding to the covariance terms between the nuclear data and the calculated quantities $\mathrm{q}^{(p)}_{\mathrm{exp},i}$. Such matrix $\mathbb{M}_{\sigma,\mathbf{c}}$ is a rectangular matrix of dimension $3n \times P$:

$$\mathbb{M}_{\sigma,\mathbf{c}} = \begin{bmatrix} \mathrm{cov}_{1,1} & \mathrm{cov}_{1,2} & \dots \\ \vdots & \ddots & \\ \mathrm{cov}_{3n,1} & & \mathrm{cov}_{3n,P} \end{bmatrix} \quad (30)$$

where

$$\mathrm{cov}_{1,2} = \frac{1}{I}\sum_{i}^{I}(\sigma 1_i - \overline{\sigma 1})(\mathrm{q}^{(2)}_{\mathrm{exp},i} - \overline{\mathrm{q}^{(2)}_{\mathrm{exp}}}) \quad (31)$$

with $\overline{\sigma 1}$ and $\overline{\mathrm{q}^{(2)}_{\mathrm{exp}}}$ defined in Eq. (2) and (14), respectively. As before, $\overline{\mathbf{ND}}$ is the prior average nuclear data and $\overline{\mathbf{ND}}'$ is the posterior distribution for the nuclear data. Similar definitions hold for their covariance matrices $\mathbb{M}_{\sigma}$ and $\mathbb{M}_{\sigma}{}'$.

4.2 Similarity with GLLS

Such description of the Mocaba equations is very similar to the one of the Generalized Linear Least Squares as it can be found for instance in Refs. [3,34]. While keeping the same notation as previously, the GLLS equations can be expressed as follows

$$\mathbf{Q_{calc,0}}' \approx \mathbf{Q_{calc,0}} + \tilde{\boldsymbol{S}}(\mathbf{ND_0'} - \mathbf{ND_0}) \quad (32)$$

$$\mathbb{M}_{\mathbf{c}}{}' = \boldsymbol{S}\mathbb{M}_{\sigma}'\boldsymbol{S}^{T} \quad (33)$$

$$\mathbf{ND_0'} = \mathbf{ND_0} + \mathbb{M}_{\sigma}\boldsymbol{S}^{T}\left(\mathbb{M}_{\mathbf{c}} + \mathbb{M}_{\mathbf{e}}\right)^{-1} \times(\mathbf{Q_{exp}} - \mathbf{Q_{calc,0}}) \quad (34)$$

$$\mathbb{M}_{\sigma}{}' = \mathbb{M}_{\sigma} - \mathbb{M}_{\sigma}\boldsymbol{S}^{\mathbf{T}}\left(\mathbb{M}_{\mathbf{c}} + \mathbb{M}_{\mathbf{e}}\right)^{-\mathbf{1}}\boldsymbol{S}\mathbb{M}_{\sigma} \quad (35)$$

with $\boldsymbol{S}$ being the matrix of the sensitivity coefficients and $\tilde{\boldsymbol{S}}$ the Jacobian matrix [34]. Different formulations can be found in the literature, but it was demonstrated in Ref. [32] that the GLLS equations can be derived from the Mocaba equations under the approximation of linear relationship between the calculated integral values and the nuclear data.
A point of importance for this work is that the GLLS method provides an update of the nominal nuclear data (called here $\mathbf{ND_0}$), whereas the updated quantities in the Monte Carlo methods are the average nuclear data ($\overline{\mathbf{ND}}$).

5 TMC, single selection and combination

The TMC method was extensively presented in many publications, and the most relevant ones in the context of this work are Refs. [29,30]. It stands for "Total Monte Carlo" and is basically used to produce the random nuclear data files. But it can also be used for simple data adjustment as presented here and it is therefore interesting in this study. But if it can provide nuclear data with better $C - E$, it does not give access to updated covariance matrices.

- Simple selection based on these files [31]: once weights are assigned to all the random files, one can simply select the random file with the highest weight. Such file can be considered as the new evaluation to be kept for a future library; it is later called "best file". This is justified since the random nuclear data files were created to cover experimental data from the EXFOR database, there is therefore a high possibility that this best file (from the point of view of integral data) is also in good

agreement with differential data. Such an assumption needs to be verified before the selected file is kept as the final evaluation. Additionally, its performance on integral benchmarks not included in the calculation of the weights needs to be verified.

- Linear combination. A slightly different approach allows to obtain extremely small $C-E$ for the integral data included in the process and is mentioned here as an interesting solution but with a poor predictive power. One can select P random files and linearly combine their integral results to obtain $C-E \simeq 0$. Let $\mathbf{X}$ be a vector of P unknowns x_p (in the present case, 14) and $\mathbb{Q}_{\rm calc}$ the integral results of a selection of P random files. The matrix $\mathbb{Q}_{\rm calc}$ has a $P \times P$ dimension with elements such as $q^{(p)}_{\rm calc,i}$, i represents the file number (as a column index) and p is the integral value (as a line index). In such case, there exists a vector $\mathbf{X}$ verifying the following equation:

$$\mathbb{Q}_{\rm calc} \times \mathbf{X} = \mathbf{Q_{exp}} \tag{36}$$

By inverting the matrix $\mathbb{Q}_{\rm calc}$, one can find the values x_p leading to $C-E=0$:

$$\mathbf{X} = {\mathbb{Q}_{\rm calc}}^{\mathbf{-1}} \times \mathbf{Q_{exp}} \tag{37}$$

There is a large possible choice of P random files and in the following, the first P files with the highest weights will be selected. As long as the $\mathbb{Q}_{\rm calc}$ can be inverted, there is always a solution. The drawback of this method is its poor predictive power for integral values not included in the procedure. Results of these selections will be presented in section 8.

6 Integration in a single ENDF file

As presented in Eq. (20) for the BMC/BFMC methods and in Eq. (28) for the Mocaba approach, the updated quantities concern the full distribution of the I values for each benchmark. This is practical from the point of view of nuclear data users seeking to reduce the calculational bias and the associated uncertainties by starting from a given nuclear data library and by including additional information, such as the integral benchmarks.

In the case of the BMC/BFMC methods, the presented approach provides a (large) number of random files with weights and a user would have to use the same random files with its own simulations and calculate weighted averages. This is certainly not practical and a different solution is proposed in the following. An alternative solution would be to use the random files having a weight higher than a certain value, so that the weighted average of the calculated integral quantity is not significantly altered. Still, if the number of relevant random files would be reduced, this remains a cumbersome solution.

From the nuclear data evaluation, such equations do not provide an adequate solution as the goal is to update the nominal quantities in $\mathbf{ND_0}$ in order to provide users a unique updated library, consisting of one single evaluated file for each isotope, containing new (posterior) cross sections and new covariance matrices.

An additional concern is that the nominal nuclear data might be different from the average of all the I random values: $\mathbf{ND_0} \neq \overline{\mathbf{ND}}$. Indeed from the variation of the model parameters, there is no constraint to assure such equality (see Ref. [35,36] for specific examples). Therefore two practical solutions are explored:

A. update (multiplying) the nominal nuclear data file $\mathbf{ND_0}$ with the ratios defined by $\overline{\mathbf{ND}}'/\mathbf{ND_0}$, effectively replacing the nominal values by the posterior averages,
B. update (multiplying) the nominal nuclear data file $\mathbf{ND_0}$ with the ratios defined by $\overline{\mathbf{ND}}'/\overline{\mathbf{ND}}$.

In the following, different results will be presented using both possibilities, referred to as update A and B. As the prior nominal nuclear data can differ from the prior average of all the random files, these two solutions are not equivalent. The first one is intuitive since it is simply a substitution of the original nuclear data by the ones providing on average better performances with the selected benchmarks. But it neglects the fact that the update was performed considering $\overline{\mathbf{ND}}$ and not $\mathbf{ND_0}$. The second solution considers that the relative change between the prior and posterior averages is the quantity to use in the update of the nominal nuclear data $\mathbf{ND_0}$. In the section 8, results from both possibilities will be presented.

7 Convergence rates

As the BMC/BFMC and Mocaba methods are based on Monte Carlo sampling of a large number of inputs (as presented, the dimension of the nuclear data vector $\boldsymbol{\sigma}$ is relatively large, higher than 10 millions), it is important that the prior and posterior quantities are converged. The convergence criterion is here very pragmatic, being that the quantities (prior and posterior nuclear data as well as integral quantities) as a function of the iteration number seem stable "by eye".

7.1 Prior quantities

Concerning the prior nuclear data, it was previously shown that $I = 10\ 000$ is enough to reach an adequate convergence for the first three moments of the probability density functions of the important nuclear data [14,11]. An example for the Monte Carlo sampling of the pdf for the prior $k_{\rm eff}$ in the case of the hmf1 (Godiva) benchmark, varying ^{235}U only, is presented in Fig. 2 top. As observed, the prior distribution for the $k_{\rm eff}$ is close to a Normal distribution and additional random cases do not significantly modify its characteristics.

7.2 Posterior quantities

The convergence of the posterior quantities is also of importance, and concerns the different $k_{\rm eff}$ or spectral indices, the updated cross sections, their uncertainties and

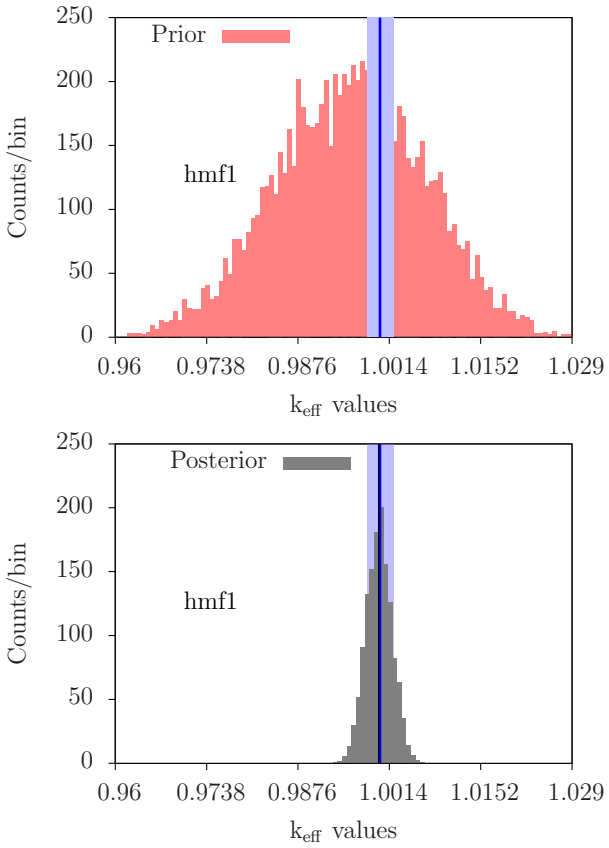

Fig. 2. Prior (top) and posterior (bottom) k_{eff} Monte Carlo sampling of the probability density function in the case of the hmf1 benchmark, varying the ^{235}U nuclear data only. The vertical line and band indicate the value of the experimental k_{eff} with its uncertainty (1.0000 ± 200 pcm). The posterior pdf is calculated with the BMC method.

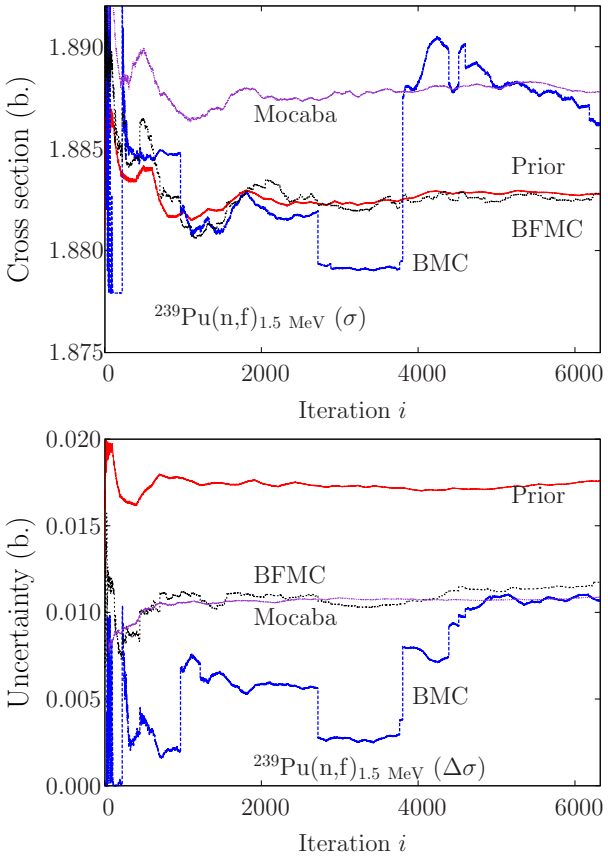

Fig. 3. Example of convergence of the ^{239}Pu(n,f) posterior cross section at 1.5 MeV (top) and its uncertainty (bottom), taking into account all benchmarks.

correlations. In the case of the BMC method, an example of a posterior pdf is presented in Fig. 2 bottom, for the same hmf1 benchmark alone. As also observed in Ref. [20], the average and standard deviation of the posterior k_{eff} distribution do not significantly vary after 1000 iterations when a single integral quantity is used.

In the application cases with many benchmarks together (see section 8), it is not practical to give such a large number of quantities and the convergence of a selection will be presented. For the posterior cross sections and their uncertainties, an example is presented in Fig. 3 in the case of the ^{239}Pu(n,f) cross section and its uncertainty at 1.5 MeV, using all the 14 integral quantities together, directly obtained from the application of above equations, without the integration in a specific ENDF-6 file. In this example, the selected cross section is of relevance for the calculation of k_{eff} and spectral indices as the neutron spectra for many benchmarks peak between 1 and 2 MeV. One can see that the cross section and its uncertainty are not significantly varying after 1000-2000 iterations for the prior, BFMC and Mocaba methods. On the contrary, strong variations can be seen in the case of BMC. Same phenomena are observed for posterior integral quantities and an example for the uncertainty on the F28/F25 spectral index for the pmf1 (Jezebel) benchmark is presented in Fig. 4. In the

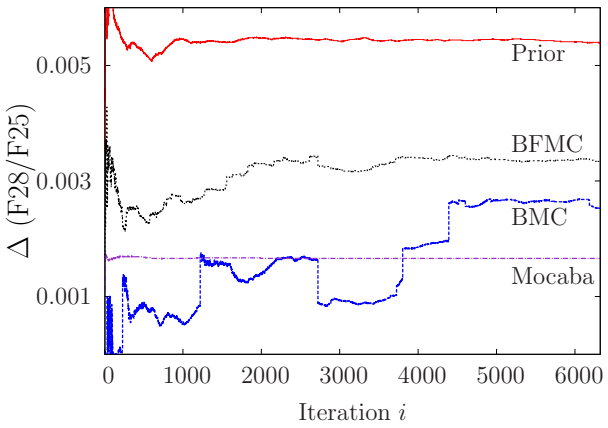

Fig. 4. Example of convergence of the prior and posterior uncertainties on F28/F25 spectral index in the case of the pmf1 benchmark, applied to the 14 integral quantities during the updating process.

case of BFMC, the uncertainty on F28/F25 still varies during a few thousands of iteration. On the contrary, the Mocaba method leads to very stable values for very small iteration numbers. Again, the BMC uncertainties strongly

vary for specific iteration numbers. It is not practical to present all the figures of convergence, but a common trend is that the Mocaba method presents less variations than the BFMC method, as a function of the iteration for the posterior nuclear data and integral quantities (see Figs. 3 and 4).

Another quantity of interest is the convergence of the standard error on the mean (SEM). In the case of unweighted sum, the SEM is estimated by the sample standard deviation divided by $\sqrt{i}$, i being the sample size. Therefore its convergence rate is proportional to $1/\sqrt{i}$. In the case of BMC/BFMC and Mocaba, their convergence rates do not follow $1/\sqrt{i}$, as weighted sums are used. A convenient way to estimate the SEM is to apply the bootstrap method [28, 37] as follows. It consists in repeating samplings in a given population, randomly replacing each time the selection to generate new data sets. In practice, the following steps are applied (as described in Ref. [28]):

- Selections of i samples are taken from the population of the calculated integral data, the number of selections is 300,
- weighted averages are calculated for each selection, for the prior, BMC/BFMC and Mocaba (in the case of the prior, a simple unweighted sum is calculated),
- the standard deviation of the 300 weighted averages (for each method) is used as an estimator of the SEM.

A representative example is presented in Fig. 5 where the SEM is calculated in the case of the pmf8 benchmark for k_{eff}, but considering the 14 integral quantities from Table 1. As observed, the estimated rate of convergence

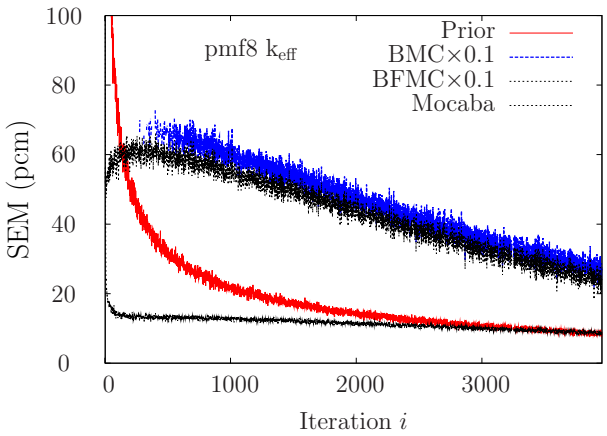

Fig. 5. Convergence of the standard error on the mean (SEM) in the case of the prior and posterior (BMC/BFMC and Mocaba) for the pmf8 benchmark with k_{eff}. In this case, the 14 integral quantities are considered in the update procedures.

for the prior is still $1/\sqrt{i}$, whereas it is closer to a linear convergence for BMC/BFMC and Mocaba for iterations above 500. It is also interesting to see that Mocaba provides the smaller SEM, and BMC/BFMC the largest. This test indicates that the BMC/BFMC and Mocaba equations do not lead to the same convergence rates for the quantities of interest. In the case of the BMC/BFMC method, the SEM of the pmf8 k_{eff} is about 600 pcm, even for high iteration numbers.

For the BMC method, the w_i can be extremely small when considering many benchmarks together: from the definitions of w_i in Eq. (18) and χ^2_i in Eq. (17), w_i can reach very small values as w_i is a product of exponentials (χ^2_i in Eq. (17) is defined as a sum). In Refs. [20,14], only one benchmark was considered (pmf1 or imf7), and the individual weights w_i were not too small: in Ref. [14], about 18 % of the weights were higher than $0.01\times w^{(\max)}$ ($w^{(\max)}$ is the maximum of all the I weights). The calculated quantities with the BMC equations cannot be reliable if too many weights are very small compared to $w^{(\max)}$. To illustrate the decrease of the w_i as a function of the number of benchmarks, Table 3 presents the number of weights being in specific ranges compared to $w^{(\max)}$, together with the correlations between two benchmarks quantities: k_{eff} of hmf28 and F28/F25 of pmf6. It becomes clear that the

Table 3. Number of weights from Eq. (18) being in a certain interval of the maximum weight $w^{(\max)}$, as a function of the number of benchmarks included in the update procedures. Also indicated are the correlation terms between k_{eff} of hmf28 and F28/F25 of pmf6.

p	$< \frac{w^{(\max)}}{1e^{10}}$ (%)	between (%)	$> \frac{w^{(\max)}}{100}$ (%)	correlation BMC	correlation Mocaba
2	7	45	48	-0.12	-0.12
3	23	58	19	-0.12	-0.12
4	32	55	13	-0.09	-0.10
5	44	47	9	-0.13	-0.09
6	44	47	9	-0.13	-0.09
7	50	44	6	-0.11	-0.09
8	78	21	1	-0.25	-0.09
9	79	20	1	-0.23	-0.05
10	92	7.6	0.4	-0.03	-0.05
14	98.2	1.8	0.1	+0.53	-0.05

weight distribution does not have enough population in the high weights to extract meaningful correlations, when the number of benchmarks is above a certain value. Such weight distribution will depend on the prior C-E values: if many $\mathbf{ND_i}$ lead to high weights for all benchmarks, then the BMC method can be used with confidence. In the present case, the correlation coefficients in Table 3 seem to be relatively stable for less than 8 benchmark values, indicating that this is the limit with the current set of selection of benchmarks and random nuclear data files. Same conclusion will hold for all posterior quantities from the BMC method: the posterior values will be very comparable to the ones for the best random file among the I cases. For uncertainties on integral values and nuclear data, they will have the tendency to be underestimated. The BFMC method attempts to solve this problem by normalizing all the χ^2 by the minimum one. As the weights are defined by the exponential of the (normalized) χ^2 in Eq. (17), their spread is much reduced compared to the one from BMC. The drawback is that these weights do not follow the principle of maximum entropy as in the case of a true Bayesian

approach [25].

As explained earlier, the results of these equations in terms of integral quantities are not the final step, as the goal is to update nominal ENDF files with the adequate nuclear data. To this end, the final quantities of interest are the integral values calculated with such posterior ENDF files (one for each isotope) using MCNP6, and their convergence rates. Again, a representative example showing the tendency as a function of iterative samples for a single benchmark, pmf8, is presented in Fig. 6 (note that for this benchmark, thorium is used as a reflector, and the thorium nuclear data are not adjusted). These k_{eff} are calculated with the posterior ^{239}Pu ENDF file, using the posterior nuclear data from method B (multiplying the nominal nuclear data file $\mathbf{ND_0}$ with the ratios defined by $\overline{\mathbf{ND}}'/\overline{\mathbf{ND}}$). As observed, both BMC and Mocaba methods seem to convergence to the experimental value with a similar convergence rate.

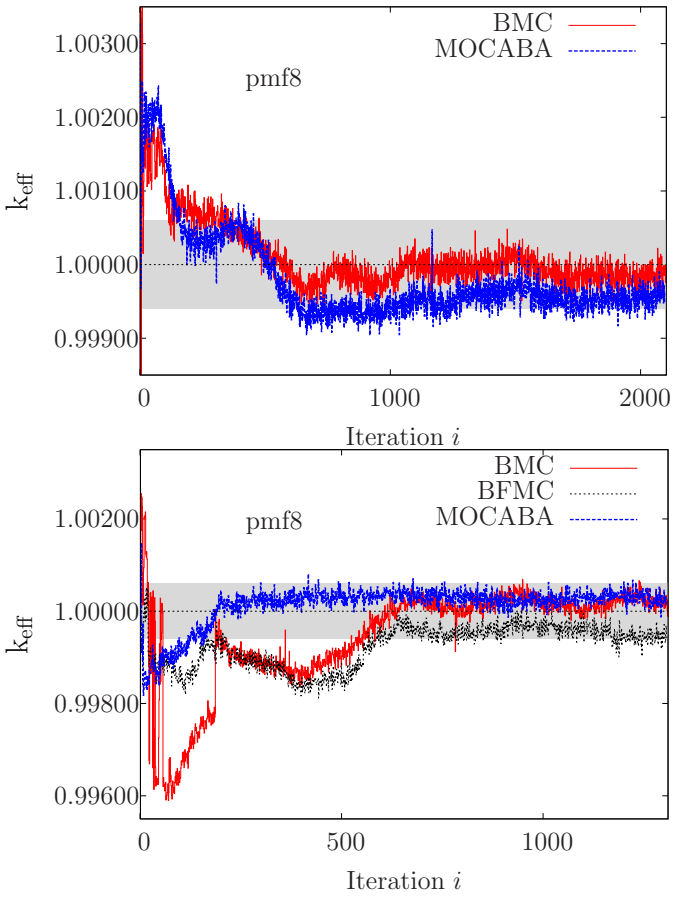

Fig. 6. k_{eff} convergence for the pmf8 benchmark (top: only the pmf8 benchmark is considered; Bottom: all benchmarks considered), using the ^{239}Pu posterior nuclear data in MCNP6 simulations.

To be more complete, such test is repeated considering all 14 integral quantities (see Fig. 6 bottom). In this case, whereas the BFMC and Mocaba methods seems to provide stable results after a few hundreds of iterations, the k_{eff} values from the BMC method can strongly vary, due to the strong variations in weights as previously observed. After these preliminary verifications of the convergence of the methods and of the posterior quantities, results with the posterior nominal ENDF files and their uncertainties will be presented in the following section.

8 Results

Before going into the example which includes many integral quantities at once, some results are presented considering a single benchmark quantity at a time. This helps to assess the performances of all methods.

8.1 Single benchmark

Results for some k_{eff} only are presented in Table 4 for the update option A. and in Table 5 for the update option B. The values $\overline{C}-E$ k_{eff} and ΔC do not change in both tables but are repeated for completeness. For all the benchmarks, the three isotopes ^{235}U, ^{238}U and ^{239}Pu are considered. The statistical uncertainty for each MCNP6 calculation is in the order of 25 pcm. In the case of single benchmark used in the adjustment processes, the BMC and BFMC methods lead to very similar results. Only the $\overline{C}-E$ for BMC are therefore presented in these tables.

Table 4. Posterior $\overline{C}-E$ k_{eff} and uncertainties for specific benchmarks, each one considered individually with the method option A. All quantities are given in pcm. Calculated values in black are within 1σ, in orange within 2σ.

	Posterior BMC Average file 0'$_A$			Posterior Mocaba Updated file 0'$_A$		
	$\overline{C}-E$	$\pm\Delta$C	C-E	$\overline{C}-E$	$\pm\Delta$C	C-E
pmf1	+11	± 195	+17	+10	± 195	+0
pmf2	+31	± 192	+27	+36	± 192	+12
pmf8	+0	± 59	-27	-1	± 60	-15
pmf22	+3	± 200	-42	+1	± 203	-33
imf1	+3	± 90	+63	+4	± 90	-118
imf2	+3	± 284	-105	+1	± 282	-101
imf7	-1	± 70	-106	-1	± 70	-48
mmf1	-1	± 160	-11	+0	± 156	-38
mmf3	+15	± 155	-13	+16	± 155	+12
$\sum\|\|/P$	8		46	8		42

As shown, both BMC and Mocaba methods succeed in individually adjusting the benchmarks for the complete adjusted distributions (see the columns $\overline{C}$-E and C-E in both tables). This is expected as the number of random files I is high enough, and the average bias is extremely small. When updating the nominal files with method A or B, the performance of the posterior files can be degraded for integral quantities, but the overall behavior is satisfactory. The absolute bias $\Sigma||/P$ is also slightly smaller

Table 5. Posterior $\overline{C}-E$ k_{eff} and uncertainties for specific benchmarks, each one considered individually with the method option B. All quantities are given in pcm. Calculated values in black are within 1σ, in orange within 2σ.

	Posterior BMC			Posterior Mocaba		
	Average		file 0'$_B$	Updated		file 0'$_B$
	$\overline{C}-E$	$\pm\Delta C$	C-E	$\overline{C}-E$	$\pm\Delta C$	C-E
pmf1	+11	± 195	+40	+10	± 195	+17
pmf2	+31	± 192	+17	+36	± 192	+59
pmf8	+0	± 59	-22	-1	± 60	-17
pmf22	+3	± 200	-8	+1	± 203	-23
imf1	+3	± 90	-3	+4	± 90	-19
imf2	+3	± 284	-38	+1	± 282	-30
imf7	-1	± 70	-72	-1	± 70	-87
mmf1	-1	± 160	+15	+0	± 156	-25
mmf3	+15	± 155	+28	+16	± 155	+53
$\sum \|\|/P$	8		27	8		37

for the method B in the case of Mocaba. Additionally, the posterior uncertainties are almost equal to the experimental uncertainties for both methods. As a conclusion of this test on a set of benchmarks (all individually considered), both methods A and B perform well for the BMC and Mocaba approach. As presented in the next section, the weight definition will differentiate the performance of the BMC and BFMC methods.

8.2 All benchmarks

To be closer to the work performed in a realistic evaluation process, the posterior nuclear data need to be produced considering many integral quantities at once. The result of these procedures can be expressed in two simple quantities: the posterior integral quantities and their covariance matrix, and the posterior nuclear data and their covariance matrix.

8.2.1 Posterior integral data and covariance matrix

For convenience, this covariance matrix is presented in the following consisting in two distinct parts: the correlation matrix and the uncertainties. The correlation factors for the Mocaba and BFMC methods are presented in Fig. 7. As mentioned, the prior correlation matrices are the same for both methods (see Fig. 1) and the correlation values for the BMC method are not reliable for this number of integral values. As before, the benchmarks are presented in 3 blocks, starting with the plutonium benchmarks, followed by the mixed and intermediate benchmarks and finally the highly enriched ^{235}U benchmarks. The following simple observations can be done:

- The correlations between the 14 integral values are reduced compared to the prior.
- Relatively strong correlations can be observed within the blocks of similar benchmarks. This is expected as they primarily contain the same isotopes,

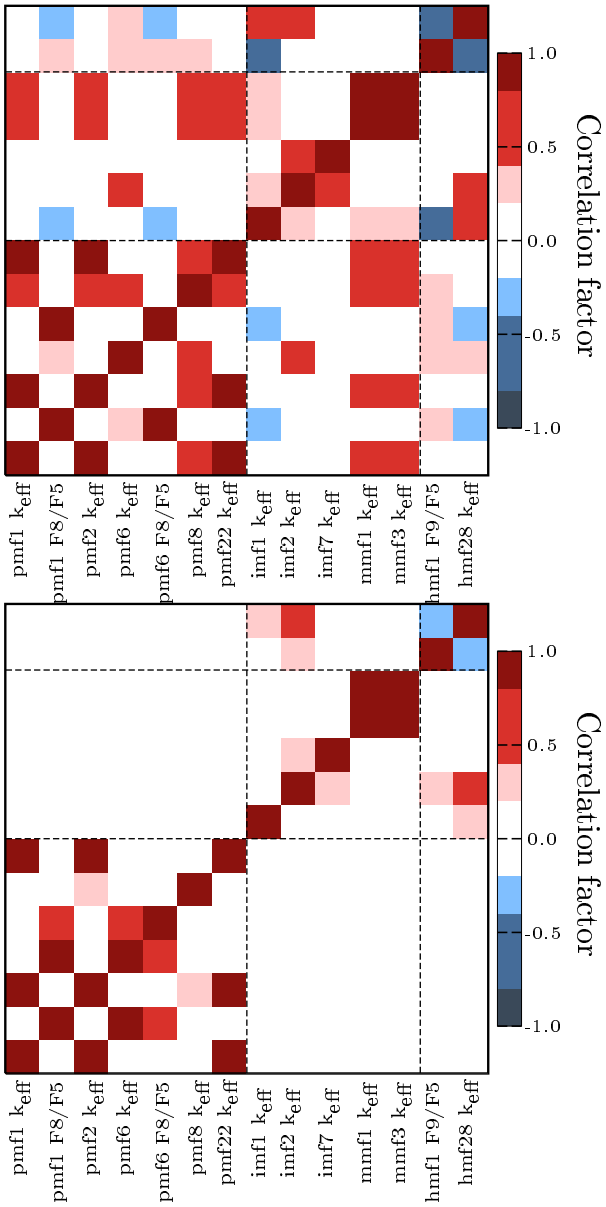

Fig. 7. Posterior correlation matrices for the 14 integral quantities for the BFMC (top) and Mocaba (bottom) methods. F8, F5 and F9 are short notations for F28, F25 and F49, respectively.

- Stronger correlations between blocks appear for the BFMC method.
- And in the case of the pmf benchmarks, the F28/F25 spectral indices are not correlated with the k_{eff} (contrary to the spectral indices of the hmf cases), as for the prior covariance matrix.

Dedicated studies to estimate correlation factors between benchmarks can be found in the literature (*e.g.* Refs. [19, 38]) and the Mocaba and BFMC approaches can certainly contribute to this field. Again, it is important to realize that correlation matrices reflect the method applied and the types of inputs, therefore differences between theses two matrices are expected. It can nevertheless be ob-

Table 6. Posterior C-E, $\overline{C}-E$ and uncertainties for all benchmarks considered together with the method option B for BMC, BFMC and Mocaba. All quantities are given in pcm. Calculated values in black are within 1σ, in orange within 2σ and in red are outside 2σ.

	Exp			Prior			Posterior BMC			Posterior Mocaba			Posterior BFMC			TMC	
				average		file 0	average		file 0'$_B$	updated		file 0'$_B$	average		file 0	best file #1834	14 files
p			ΔE	$\overline{C}-E$	$\pm\Delta$C	C-E	$\overline{C}-E$	$\pm\Delta$C	C-E	C-E	$\pm\Delta$C	C-E	$\overline{C}-E$	$\pm\Delta$C	C-E	C-E	C-E
1	imf1	k_{eff}	90	-91	± 910	+363	-100	± 95	-136	-12	± 84	-218	-6	± 232	+165	+22	+18
2	imf7	k_{eff}	70	-292	± 850	-153	+12	± 80	-94	-1	± 69	-193	-19	± 191	-116	+39	+14
3	mmf1	k_{eff}	160	-132	± 670	+3	-112	± 95	-168	-117	± 98	-87	-118	± 196	-129	-72	+25
4	pmf2	k_{eff}	200	+329	± 670	+440	+290	± 115	+157	+354	± 84	+399	+447	± 165	+397	+574	+25
5	pmf1	k_{eff}	200	+77	± 780	+162	-23	± 142	-124	+55	± 106	+153	+171	± 200	+129	+413	+28
6	pmf1	F8/F5	230	-394	± 540	-230	-145	± 138	-220	-68	± 167	-40	-55	± 323	-40	-240	+9
7	mmf3	k_{eff}	160	+117	± 640	+280	+169	± 78	+68	+160	± 87	+136	+159	± 179	+61	+151	+23
8	hmf1	F9/F5	1400	-2680	± 2530	-2730	-1107	± 620	-1240	-867	± 827	-780	-1555	± 1270	-1630	-1060	+34
9	pmf22	k_{eff}	210	-85	± 796	+13	-152	± 120	-310	-86	± 109	-37	+23	± 207	-19	+220	+24
10	hmf28	k_{eff}	300	+309	± 932	+686	+163	± 115	+124	+116	± 155	+2	+274	± 298	+263	+62	+9
11	imf2	k_{eff}	300	-238	± 835	+8	-90	± 141	-218	-111	± 138	-367	-5	± 237	-112	+25	+11
12	pmf6	k_{eff}	300	+478	± 777	+559	+569	± 221	+453	+393	± 194	+490	+561	± 310	+565	+144	+13
13	pmf6	F8/F5	200	-301	± 424	-40	+29	± 114	-210	+80	± 136	-120	+110	± 256	-120	-40	+14
14	pmf8	k_{eff}	60	-192	± 734	-126	-32	± 38	-206	-43	± 56	-206	-69	± 145	+83	-125	+26
	$\sum\|\|/P$	(pcm)		414	± 480	414	214	± 67	287	176	± 75	249	272	± 147	292	207	18
	$\sum/P$	(pcm)		-54	± 480	-55	-38	± 67	-182	-11	± 75	-76	-35	± 147	-63	+10	+18
	χ^2/P			3.3		3.0	0.8		1.5	0.6		2.2	0.9		1.2	1.3	0.02

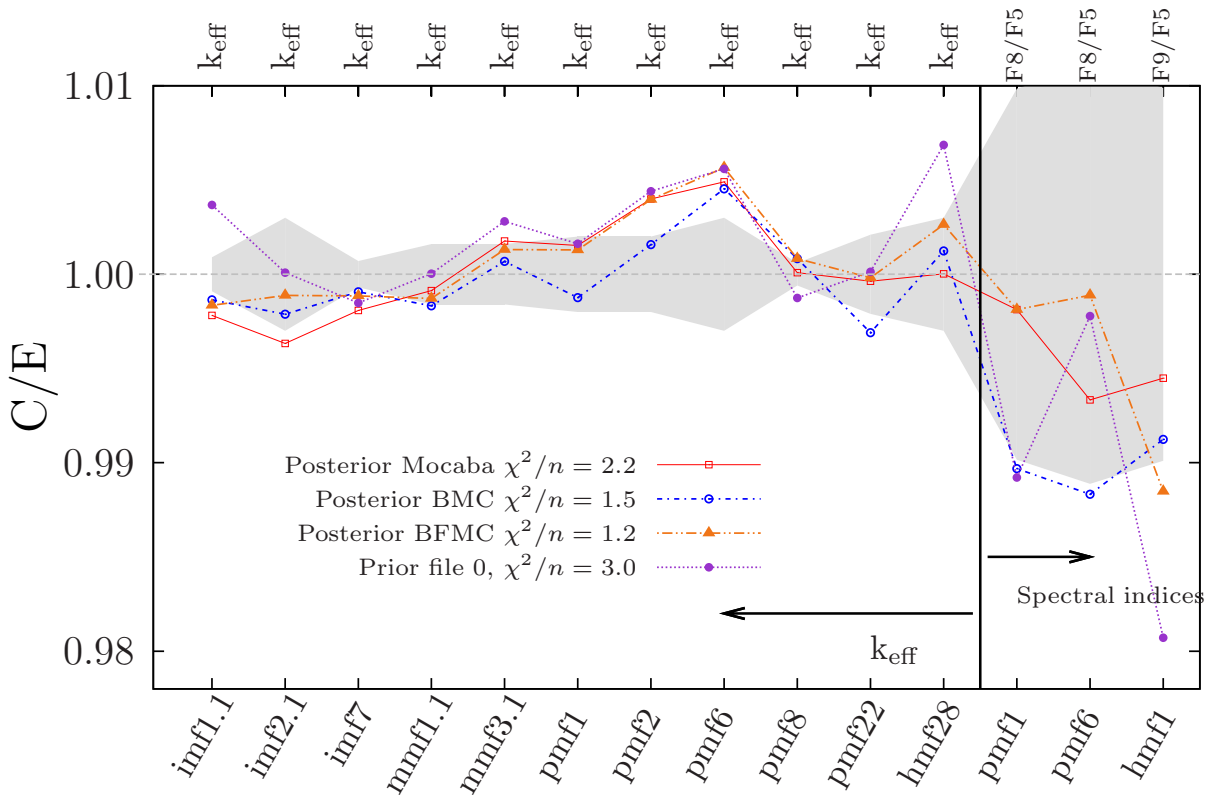

Fig. 8. C/E comparisons for data from Table 6. The gray band is the experimental uncertainty.

served that these two matrices are similar: one presenting stronger correlations than the other, but the signs of the correlations values are conserved.
The results for the uncertainties are presented in Table 6, using method B for BMC, BFMC and Mocaba (the results for method A are very similar and are not presented here). As observed, the posterior distributions and the update "file $0'_B$" provide in general better agreement with the experimental values, compared to the prior. Without surprise, the combination of the 14 random files with the factor $\mathbf{X}$ from Eq. (37) provides better results. All goodness of fit estimators presented at the bottom of Table 6 indicate an improvement of the calculated values. Apart from the combination of 14 files, the best results are obtained directly after the application of the update methods, without implementing the changes in an ENDF-6 file; but from a practical point of view, the posterior ENDF-6 files from both methods will eventually be given a nuclear data library. Therefore the relevant results in this study are the performances of the posterior ENDF-6 files. A degradation of performances can be observed compared to the results of the different equations, but the results still show sizable improvements compared to the prior. The simple method of extracting the best file from the random set performs very well compared to the other methods. One of its drawbacks is nevertheless that it does not allow to obtain posterior covariance matrices for the nuclear data. From the other methods however, the calculated uncertainties are strongly reduced. The posterior uncertainties are always smaller than the prior ones, and it can be observed that the BMC uncertainties are in most cases smaller than the Mocaba and BFMC uncertainties. This is linked to the fact that too many weights w_i are extremely small, therefore the BMC method tends to provide results driven by a very small amount of random files having the highest weights. The BFMC also systematically gives uncertainties larger than Mocaba. This could be mitigated by using the original [27] BFMC definition of weight, which uses a an additional square and produces narrower distributions. This is important for the selection of covariance matrices to be inserted in a nuclear data library.
Values presented in Table 6 are plotted in Fig. 8 in terms of C/E, with the experimental uncertainties. For all methods except the combination of 14 random files, some calculated integral quantities are outside one sigma experimental uncertainty (7 for BMC, BFMC and Mocaba, and 5 for the TMC best file). This can be partly attributed to the presence of other isotopes for which the cross sections are considered fixed during the adjustment procedure, as for pmf2 (containing 20 % of ^{240}Pu). Also, the considered random files contain some "*stiffness*" due to the nuclear reaction models: some cross sections globally keep the same shape among all random files, and only vary in amplitude (as for capture cross sections). This indicates the importance of having prior distributions not only covering all possible cross section values, but also allowing for local shape deformation (about the stiffness obtained from specific reaction model, see Ref. [39]). Finally, the updates of the nuclear data are applied to specific energy groups. Even if this energy structure is relatively fine above the resonance range, it certainly leads to some approximation.

8.2.2 Cross section covariance matrix

From the evaluation point of view, the quantities of interest are the nuclear data (in the present case: cross sections, $\overline{\nu}$ and the prompt fission neutron spectra). The posterior cross sections used in the ENDF-6 files with the MCNP6 calculations need to be in agreement with other sources of information (such as EXFOR), *i.e.* the posterior values shall not be too different compared to the prior nominal cross sections. The ratios of the most important cross sections and $\overline{\nu}$ are presented in Fig. 9 for the three isotopes of interest, for the BMC/BFMC and Mocaba methods. These ratios represent the posterior cross sections as used in the ENDF-6 files (with the method B) divided by the cross section of the unperturbed file number 0 (or nominal file). The first remark is that these ratios are different in amplitude between Mocaba (or BFMC) and BMC, although the shapes are similar. One has to keep in mind that the BMC posterior cross sections suffer from the "*curse of low weights*", which tends to make the posterior cross sections very close to the ones from the random runs having the highest weights. Therefore the plotted ratios in the case of BMC do not represent the combination of many random cross sections for the posterior, but rather an average of a few cross sections. The second remark is that the cross section changes in the case of Mocaba and BFMC are very similar and all relatively small, less than 5 % with a maximum change for the ^{239}Pu(n,el) cross section. This gives some confidence in the posterior cross sections, as many of them are believed to be well known in the libraries such as JEFF, JENDL of ENDF/B. A detailed study of these variations is not necessary here and would be part of the general evaluation process, including comparisons between libraries, experimental data and possibly information from other integral results. It is worth mentioning that a previous study comparing BFMC and the Kalman method indicates a difference in the uncertainty reduction of a factor 2, BFMC providing larger uncertainties [40]. This is similar to the ratios for some of the presented uncertainties between Mocaba and BFMC in Fig. 9. One can notice that the $\overline{\nu}$ for ^{235}U is slightly reduced, as the prior k_{eff} for the hmf28 benchmark is too high by almost 700 pcm (only benchmark where $\overline{\nu}$ of ^{235}U play a dominant role, see Fig. 9). This denotes the importance of selecting a representative set of benchmarks, as the posterior ^{235}U nuclear data are likely to also reduce the k_{eff} of benchmarks not included in this process. In a real case scenario, more highly enriched ^{235}U systems will be considered.
A comparison between posterior and prior uncertainties is also presented in Fig. 9. Again, the results from the BMC method are not reliable because of the weight distribution which tends to reduce the uncertainties to zero. In the case of Mocaba, the uncertainty reduction is not negligible, reflecting the integral uncertainty reduction (in combination with the posterior cross section correlations).

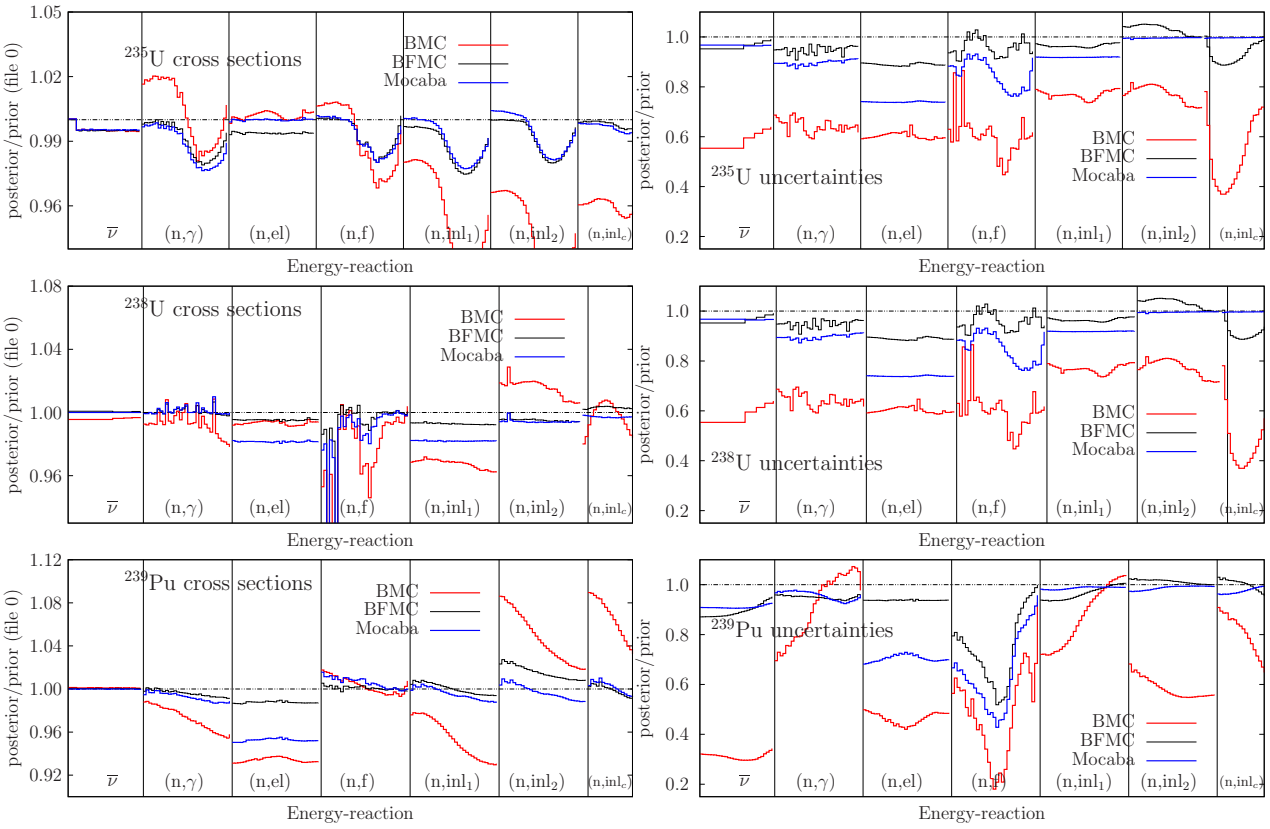

Fig. 9. Posterior ^{235,238}U and ^{239}Pu cross sections and $\overline{\nu}$ (left) and uncertainties (right) for considering all 14 integral quantities from the 12 benchmarks. In each rectangle the X-axis represents the incident neutron energy from 100 keV to 6 MeV.

The strongest reduction concerns the fission cross sections of ^{235}U and ^{239}Pu. This is partially due to the fact that the prior uncertainties were on purpose very large; this reduction needs to be seen relatively to the other experimental uncertainties such as those coming from EXFOR. This is typically the work performed during an evaluation process and is not the subject of this work. The results only confirm that the proposed procedures provide sensible cross section updates. The uncertainty reduction for BFMC is the smallest of the three methods. Such changes (together with the posterior nuclear data correlations) still allow to globally reduce the benchmark uncertainties by almost a factor of 3 (see Table 6).

The last quantity to monitor is the posterior correlation matrix for the nuclear data. Such matrices were already presented in Refs. [20,14] for ^{239}Pu and ^{235,238}U independently, and the present benchmark selection allows to obtain cross-correlations between these three isotopes. Fig. 10 presents such correlations in the case of the BFMC method. Three large blocks are visible, one for each isotope. Inside these blocks, smaller ones represent specific reactions with the X and Y-axis being the incident neutron energy from 4 keV to 20 MeV, except for the prompt fission spectra, where the axis represent the outgoing neutron energies.

As in the case of the previous publications, the prior correlation matrix does not include cross-isotope correlation, and such correlations appear due to the integral data. It is certainly too long to have an exhaustive study of these correlations, but one can notice the anti-correlation between $\overline{\nu}$ and (n,f) for ^{239}Pu, and between $\overline{\nu}$ for ^{239}Pu and ^{235}U (see Ref.[14] for more detailed descriptions). These correlations play a role in the decrease of the calculated uncertainties for the integral quantities. Their relative importance compared to the decrease of the nuclear data uncertainties will have to be quantified in another study.

8.3 Predictive power

As demonstrated, the posterior nuclear data obtained with the different methods produce improved $C-E$ for the integral quantities included in the different processes. This is achieved without strongly changing the nuclear data themselves, but it also allows a reduction of calculated uncertainties. The final question studied here concerns the testing of the posterior nuclear data files with integral quantities not included in the updating procedure (so-called "target experiment"). Different ENDF-6 files will be tested with a new set of criticality benchmarks: the prior nominal file (file 0), the posterior files (BMC, BFMC and Mocaba) and the best prior file (file 1834). 51 benchmarks are used: 18 hmf, 18 pmf, 7 imf, 3 mmf, 4 mcf and 1 icf (mcf and icf stand for mixed and intermediate fuel in compound form under a fast neutron spectrum, respectively. A mixed fuel contains both uranium and plutonium, whereas

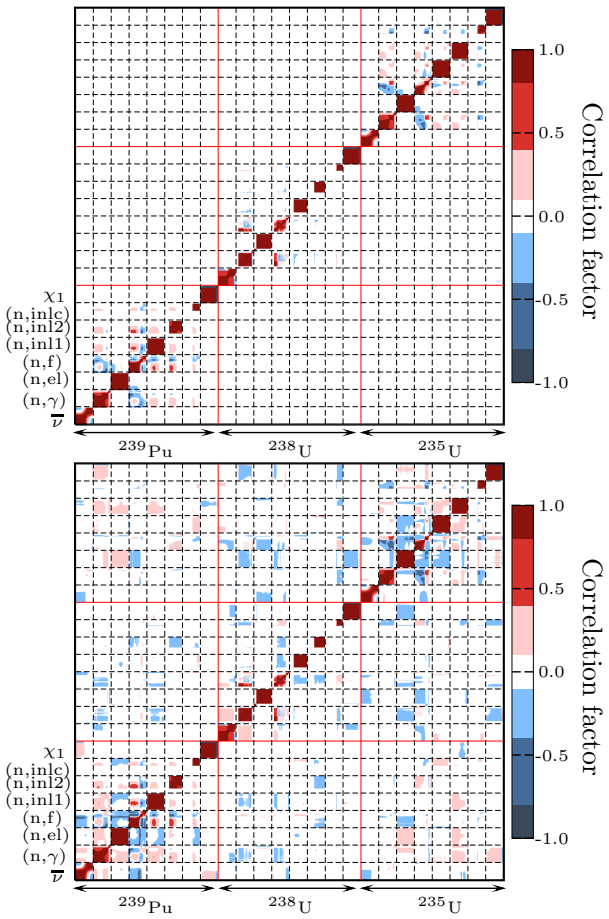

Fig. 10. Prior (top) and posterior (bottom) correlation matrices in the case of the BFMC method for the 14 integral quantities. The prompt fission neutron spectra are represented by the letter χ_1 for the incident neutron energy of 0.5 MeV.

an intermediate fuel does not contain plutonium but both ^{235}U and ^{238}U in appreciable amount). In the case of the combination of the 14 files, the **X** values lead to negative k_{eff} for some benchmarks. This is expected as this method is a simple fit without any predictive power. The goodness of fit estimators are therefore not presented, knowing that such combination cannot be used in the evaluation process.

One should first notice that the adjustment of ^{235}U is mainly driven by the hmf28 benchmark, being the only highly enriched ^{235}U benchmark for k_{eff}. As the prior C are almost 700 pcm above the E value, the effect of the adjustment is to reduce either $\overline{\nu}$ or (and) the fission cross section (see Fig. 9). Therefore it is expected that the calculated k_{eff} values for the new benchmarks are lower than the values from the file 0. Results are presented in Table 7 for different categories of benchmarks.

As observed, the best performances are obtained for the prior nominal file 0. The adjustment methods as well as the best random file lead to larger χ^2 and biases. Such conclusion is dependent on the selection of benchmarks and on the type of random files used, but it still demonstrates that an adjustment is firstly valid for a given number of systems, and that any use of the adjusted nuclear data outside this selection has to be checked.

Such observations do not discard the advantages of the presented methods for the uncertainty reduction, but it puts some light on the limit of the presented approach.

Table 7. Predictive power with additional benchmarks not included in the adjustment procedures. 51 benchmarks are used: 18 hmf, 18 pmf, 7 imf, 3 mmf, 4 mcf and 1 icf. Results are expressed in pcm, except for the χ^2.

	File 0	BMC	BFMC	Mocaba	Best 1834
	All benchmarks				
$\sum \|\|/P$	311	627	493	470	423
$\sum /P$	+117	+153	+19	-37	-162
χ^2/P	3.2	13.3	9.2	8.4	7.5
	hmf benchmarks				
$\sum \|\|/P$	272	654	605	654	702
$\sum /P$	-105	-641	-590	-641	-702
χ^2/P	2.4	14.3	12.9	14.3	16.0
	pmf benchmarks				
$\sum \|\|/P$	300	639	413	369	227
$\sum /P$	+190	+639	+370	+344	+159
χ^2/P	3.3	11.8	6.1	4.8	2.2
	other benchmarks				
$\sum \|\|/P$	373	582	449	371	323
$\sum /P$	+296	+468	+351	+230	+101
χ^2/P	4.1	14.2	8.4	5.6	3.4

9 Discussion

This study on the possibility of using specific Monte Carlo adjustment methods with integral quantities allowed to quantify some advantages and drawbacks, taking into account the aspect of the evaluation of nuclear data. Some positive outcomes can be mentioned such as (1) the ability with the BFMC and Mocaba methods to produce posterior nuclear data evaluation files with improved performances compared to the prior, and (2) the possibility to reduce the calculated benchmark uncertainties by reasonably reducing nuclear data uncertainties and using cross isotope correlations. It also pointed out the limit of the BMC method with the necessity to have a sufficient number of relevant weights.

Nevertheless, some improvements are still needed, such as

- Relevant choice of benchmarks. In this study, a limited number of benchmarks were used, mostly based on the k_{eff} quantity. For a real-case application, other sources of data need to be considered, such as activation and shielding benchmarks (*e.g.* from the SINBAD database), reactor benchmarks (from the IRPHE and SFCOMPO databases), and possibly any other sources of trusted data. This will allow to span a larger field of application, hopefully improving the prediction power of the adjusted evaluations.
- Better reaction models. As it was pointed out, the set of random files used in this work is based on reaction

models which produce rigid cross sections (the shape of some cross sections is basically not changed, while only the amplitude is varying). This is therefore reducing the range of possibilities for integral calculations. One convenient solution is to produce random files based on different models, such as different level density models. This has to be explored in the future, understanding that this type of changes can produce very different cross sections, leading to additional parameter adjustments for the prior distributions.

- Perform such study in the model parameter space. Instead of adjusting nuclear data (cross sections, $\overline{\nu}$, spectra), one can directly propagate the adjustment to the model parameters. Once such posterior parameter distributions are obtained, one can produce the corresponding nuclear data. This solution will be especially relevant in the resolved resonance range where the cross section energy grid is extremely dense. Such possibility also needs to be explored.
- Directly include EXFOR data in the adjustment process. Instead of using integral data for the adjustment, one can also include differential data from the EXFOR database. The only caution is to avoid so-called "double counting": using the differential data before the adjustment process to obtain a range of model parameters, and then to use these data again during the adjustment.
- Use of a generalized χ^2 definition. Since the principle of maximum likelihood, on which the $\exp(-\chi^2_i)$ weight of the BMC is based, is perhaps the most fundamental used statistical concept here, a solution is probably to be found in the definition of χ^2. The limitations of using a "naive" χ^2 for differential data is given in Ref. [21]. The same holds for integral data. We often can do nothing else than assume that we have a model prediction (in this case a k_{eff} calculation) and well-establish experimental data and their uncertainties. It is not difficult to see that adding uncorrelated experimental information (*e.g.* another integral benchmark) to the χ^2 definition will only lower the weight if it is assumed uncorrelated with the rest, leading to very small numbers of the weights in the Bayesian update. On top of that, hidden model deficiencies are not taken into account (should always a nuclear data library + criticality calculation lead to a perfect description) as well as errors in the experimental data (in addition to their uncertainties). In other words, widely varying, very small w_i weights may indicate that we are comparing the wrong things rather than that $\exp(-\chi^2)$ is not a good indicator.

Apart from these practical and unexplored possibilities, some other questions remain opened. The first one concerns the production of a complete evaluated file, allowing to reduce the calculated uncertainty on integral quantities and to obtain better $C-E$. As presented, none of the adjustment methods fulfill both these goals. A possibility is therefore to keep the nominal nuclear data from file 0 (best estimate) and to add an adjusted covariance matrix, for instance from the BFMC method. This will allow to obtain the best $C-E$, and to reduce uncertainties. The drawback might be that there is a loss of consistency between the nominal values and the covariance matrix, but one can argue that this is already the case in most of the general-purpose libraries.

The second question to be answered is about the necessity to include integral experiments in the evaluation process. As presented in the introduction, there is a need for reducing calculated uncertainties on integral quantities, and by including some integral benchmarks in the evaluation process, such a goal is achieved. But there might be other means to reduce the nuclear data uncertainties without explicitly using integral data, as for instance using more constraints from nuclear reaction modeling. Such an example exists for the ^{238}U(n,inl) reaction included in the ENDF/B-VIII library where a better modeling allowed to significantly reduce the uncertainties of these cross section. Some questions still remain on the validity of such approach, but it offers an alternative solution.

10 Conclusion

In this paper, we have explored the possibilities to apply different Monte Carlo adjustment methods (1) to improve the agreement between calculated and measured integral quantities, and (2) to reduce the calculated uncertainties on these values. As it was presented, the BFMC and Mocaba methods fulfill these goals for the selected benchmarks. This study therefore demonstrates the applicability of these Monte Carlo methods, but also indicates their limits regarding the predictive power in terms of biases. Still, the reduction of uncertainties is successfully demonstrated and some future possibilities are presented.

References

1. N. Otuka *et al.*, Towards a More Complete and Accurate Experimental Nuclear Reaction Data Library (EXFOR): International Collaboration Between Nuclear Reaction Data Centres (NRDC), Nucl. Data Sheets **120** (2014) 272.
2. J.B. Briggs Ed., International Handbook of evaluated Criticality Safety Benchmark Experiments, NEA/NSC/DOC(95)03/I, 2004, Organization for Economic Co-operation and Development, Nuclear Energy Agency.
3. Assessment of Existing Nuclear Data Adjustment Methodologies, A report by the Working Party on International Evaluation Co-operation of the NEA Nuclear Science Committee, WPEC-33, NEA/NSC/WPEC/DOC(2010)429, OECD, 2011.
4. G. Palmiotti and M. Salvatores, Developments in Sensitivity Methodologies and the Validation of Reactor Physics Calculations, Science and Technology of Nuclear Installations, Volume 2012 (2012), Article ID 529623,
5. M. Aufiero, M. Fratoni, G. Palmiotti and M. Salvatores, Continuous Energy Cross Section Adjustment: a New Method to Generalize Nuclear Data Assimilation for a Wider Range of Applications, International Conference

on Mathematics & Computational Methods Applied to Nuclear Science & Engineering, Jeju, Korea, April 16-20, 2017, on USB (2017).
6. C. de Saint Jean, P. Archier, E. Privas and G. Noguère, On the use of Bayesian Monte-Carlo in evaluation of nuclear data, EPJ Web of Conferences **146** (2017) 02007.
7. S. Pelloni, Comparison of progressive incremental adjustment sequences for cross-section and variance/covariance data adjustment by analyzing fast-spectrum systems, Annals of Nuclear Energy **106** (2017) 33.
8. S. Pelloni and D. Rochman, Cross-section adjustment in the fast energy range on the basis of an Asymptotic Progressing nuclear data Incremental Adjustment (APIA) methodology, Annals of Nuclear Energy **115** (2018) 323.
9. M. Salvatores *et al.*, Methods and Issues for the Combined Use of Integral Experiments and Covariance Data: Results of a NEA International Collaborative Study, Nucl. Data Sheets **118** (2014) 38.
10. C. de Saint Jean, P. Archier, E. Privas, G. Noguère, O. Litaize and P. Leconte, Evaluation of Cross Section Uncertainties Using Physical Constraints: Focus on Integral Experiments, Nucl. Data Sheets **123** (2015) 178.
11. A.J. Koning and D. Rochman, Modern nuclear data evaluation with the TALYS code system, Nucl. Data Sheets **113** (2012) 2841.
12. A. Trkov, M. Herman and D. A. Brown, ENDF-6 Formats Manual, CSEWG Document ENDF-102, Report BNL-90365-2009 Rev.2, Brookhaven National Laboratory, October 2012.
13. R.E. MacFarlane and A.C. Kahler, Methods for processing ENDF/B-VII with NJOY, Nuclear Data Sheets **111** (2010) 2739.
14. D. Rochman, E. Bauge, A. Vasiliev, H. Ferroukhi and G. Perret, Nuclear data correlation between different isotopes via integral information, submitted to EPJ/N, August 2017.
15. J. Dyrda, N. Soppera, I. Hill, M. Bossant and J. Gulliford, New features and improved uncertainty analysis in the NEA nuclear data sensitivity tool (NDaST), EPJ Web of Conferences **146** (2017) 06026.
16. M. Ishikawa, Application of Covariances to Fast Reactor Core Analysis, Nucl. Data Sheets **109** (2008) 2778.
17. E. Peters, F. Sommer, M. Stuke, Modeling of critical experiments and its impact on integral covariance matrices and correlation coefficients, Annals of Nuclear Energy **92** (2016) 355.
18. T. Ivanova, E. Ivanov and G.E. Bianchi, Establishment of Correlations for Some Critical and Reactor Physics Experiments, Nuclear Science and Engineering **178** (2017) 311.
19. E. Alhassan, H. Sjostrand, P. Helgesson, M. Osterlund, S. Pomp, A.J. Koning and D. Rochman, Selecting benchmarks for reactor simulations: An application to a lead fast reactor, Annals of Nuclear Energy **96** (2016) 158.
20. D. Rochman, E. Bauge, A. Vasiliev and H. Ferroukhi, Correlation nu-sigma-chi in the fast neutron range via integral information, European Journal of Physics **N 3** (2017) 14.
21. A.J. Koning, Bayesian Monte Carlo method for nuclear data evaluation, Eur. Phys. J. **A 51** (2015) 184.
22. E. Bauge, G. Bélier, J. Cartier, A. Chatillon, J.M. Daugas, J.P. Delaroche, P. Dossantos-Uzarralde, H. Duarte, N. Dubray, M. Ducauze-Philippe, L. Gaudefroy, G. Gosselin, T. Granier, S Hilaire, Huu-Tai P. Chau, J.M. Laborie, B. Laurent, X. Ledoux, C. Le Luel, V. Méot, P. Morel, B. Morillon, O. Roig, P. Romain, J. Taieb, C. Varignon, N. Authier, P. Casoli, B. Richard, Coherent investigation of nuclear data at CEA DAM: Theoretical models, experiments and evaluated data, Eur. Phys. J. A **48** (2012) 113.
23. E. Bauge, M. Dupuis, S. Hilaire, S. Péru, A.J. Koning, D. Rochman, S. Goriely, Connecting the Dots, or Nuclear Data in the Age of Supercomputing, Nucl. Data Sheets **118** (2014) 32.
24. R. Capote, D.L. Smith, A. Trkov and M.Meghzifene, A new formulation of the Unified Monte Carlo Approach (UMC-B) and cross-section evaluation for the dosimetry reaction ^{55}Mn(n,γ)^{56}Mn, Journal of ASTM International **9** (2012) 1.
25. D.L. Smith, A Unified Monte Carlo Approach to Fast Neutron Cross Section Data Evaluation, Proceedings of the 8$^{\text{th}}$ International Topical Meeting on Nuclear Applications and Utilization of Accelerators, Pocatello, July 29 August 2, 2007, p. 736.
26. P. Helgesson, H. Sjöstrand, A.J. Koning, J. Ryden, D. Rochman, E. Alhassan and S. Pomp, Combining Total Monte Carlo and Unified Monte Carlo: Bayesian nuclear data uncertainty quantification from auto-generated experimental covariances, Progress in Nuclear Energy **96** (2017) 76.
27. E. Bauge, "Full Model" Nuclear Data and Covariance Evaluation Process Using TALYS, Total Monte Carlo and Backward-forward Monte Carlo Nucl. Data Sheets **123** (2015) 201.
28. D.F. Gatz and L. Smith, The standard error of a weighted mean concentration -I. Boostrapping vs. other methods, Atmospheric Envir. **29** (1995) 1185.
29. D. Rochman and A.J. Koning, How to randomly evaluate nuclear data: a new method applied to ^{239}Pu, Nucl. Sci. and Eng. **169** (2011) 68.
30. D. Rochman and A.J. Koning, Improving the H in H_2O thermal scattering data using the Petten method, Nucl. Sci. and Eng. **172** (2012) 287.
31. D. Rochman and A.J. Koning, Evaluation and adjustement of the neutron-induced reactions of ^{63,65}Cu, Nucl. Sci. and Eng. **170** (2012) 265.
32. A. Hoefer, O. Buss, M. Hennebach, M. Schmid and D. Porsch, MOCABA: A general Monte Carlo-Bayes procedure for improved predictions of integral functions of nuclear data, Annals of Nuclear Energy **77** (2015) 514.
33. T. Watanabe, T. Endo, A. Yamamoto, Y. Kodama, Y. Ohoka and T. Ushio, Cross section adjustment method based on random sampling technique, Jour. of Nucl. Sci. and Techno. **51** (2014) 590.
34. S. Pelloni, Application of an iterative methodology for cross-section and variance/covariance data adjustment to the analysis of fast spectrum systems accounting for nonlinearity, Annals of Nuclear Energy **72** (2014) 373.
35. D. Rochman, A.J. Koning, and S.C. van der Marck, Exact nuclear data uncertainty propagation for fusion neutronics calculations, Fusion Engineering and Design **85** (2010) 669.
36. D. Rochman, A.J. Koning, and S.C. van der Marck, Uncertainties for criticality-safety benchmarks and k_{eff} distributions, Annals of Nuclear Energy **36** (2009) 810.
37. B. Efron and R. Tibshirani, Statistical data analysis in the computer age, Science **253** (1991) 390.
38. A. Vasiliev, D. Rochman, M. Pecchia, H. Ferroukhi, Exploring Stochastic Sampling in Nuclear Data Uncertainties Assessment for Reactor Physics Applications and Validation Studies, Energies **9** (2016) 1039.

39. M.T. Pigni, M. Herman, P. Oblozinsky, and F.S. Dietrich, Sensitivity analysis of neutron total and absorption cross sections within the optical model, Phys. Rev. **C83** (2011) 24601.
40. M.B. Chadwick T. Kawano, P. Talou, E. Bauge, P. Dossantos-Uzarralde and P.E Garett, Yttrium ENDF/B-VII Data from Theory and LANSCE/GEANIE Measurements and Covariances Estimated using Bayesian and Monte-Carlo Methods, Nucl. Data Sheets **108** (2007) 2742.